Stepwise dissociation of ion pairs by water molecules: cationdependent separation mechanisms between carboxylate and alkali-earth metal ions †

Jeremy Donon, Jean-Xavier Bardaud, Valérie Brenner, Shun-Ichi Ishiuchi, Masaaki Fujii, Eric Gloaguen

COMMUNICATION

Stepwise dissociation of ion pairs by water molecules: cation-dependent separation mechanisms between carboxylate and alkali-earth metal ions†

Received 00th January 20xx,
Accepted 00th January 20xx

DOI: 10.1039/x0xx00000x

Jeremy Donon,[a] Jean-Xavier Bardaud,[a] Valérie Brenner,[a] Shun-Ichi Ishiuchi,[b,*] Masaaki Fujii,[b,*] Eric Gloaguen[a,*]

Michrohydrated H_2-tagged ion pairs $(Ca^{2+}, AcO^-)(H_2O)_{n=0-8}$ and $(Ba^{2+}, AcO^-)(H_2O)_{n=0-5}$ are investigated by IR photodissociation laser spectroscopy and DFT-D frequency calcualtions. The detailed picture of the first steps of ion dissociation reveals two mechanisms, where water molecules promote dissociation either directly or indirectly depending on the nature of the cation.

Ion dissociation and pairing are ubiquitous phenomena occurring in electrolytes,[1] including biological media.[2] Despite numerous experimental studies in solution, identifying the supramolecular structure of paired ions together with their surrounding solvent molecules is often a challenging task.[3, 4] Pairing between acetate and alkali cations in aqueous solution is a prototypical example,[5] where structure elucidation is often limited to the characterization of solvent-shared vs. contact ion pairs.[6-8] A few rare studies managed to push further the interpretation of experimental data at the cost of an advanced theoretical work with explicit solvation.[9, 10]

In addition to these studies in solution, the investigation of ion pairs in gas-phase experiments provide a unique opportunity to decompose, and thus better understand, the processes at play in ion pairing.[11-16] In particular, microsolvation experiments,[13, 14, 16-20] where a controlled number of water molecules are attached to an ion pair, provide valuable information on the role played by the first surrounding water molecules on the supramolecular structure, and have been applied to investigate the pairing properties of the carboxylate group.[18-20] Recently, a series of IR spectra of deuterated propionate attached to both a doubly-charged calcium atom and an increasing number of water molecules $(Ca^{2+}, d\text{-}PrO^-)(H_2O)_{n=0-12}$ enabled Denton et al. to elegantly reveal the microsolvation scheme of this ion pair up to a relatively large number of water molecules.[20] However, these experiments are quite challenging and very few microsolvation schemes of ion pairs are currently known.

Taking advantage of the potential of such an approach, the present work aims at revealing the role of water molecules in the ion dissociation involving cations of different nature, *i.e.* Ca^{2+} and Ba^{2+}. Their different ionic radius (100 vs. 135 pm respectively)[21] is expected to lead to different ion pairing properties as rationalized by Collins et al. who compared the surface charge density of several cations: Ca^{2+} has a strong propensity to form contact ion pairs with carboxylate groups whereas Ba^{2+}, with a smaller surface charge density similar to that of Na^+, has a relatively smaller pairing inclination.[22]

IR photodissociation spectra of H_2-tagged calcium and barium acetate microsolvated clusters, *i.e.* $(Ca^{2+}, AcO^-)(H_2O)_{n=0-8}$ (Fig. 1) and $(Ba^{2+}, AcO^-)(H_2O)_{n=0-5}$ (Fig. 2) have been recorded in the carboxylate symmetric and antisymmetric stretches ($\nu_s(CO_2^-)$ and $\nu_a(CO_2^-)$) as well as water bending $\delta(H_2O)$ spectral ranges in order to compare their respective microsolvation schemes. While transitions above 1575 cm^{-1} can be readily assigned to $\delta(H_2O)$, couplings of $\nu(CO_2^-)$ with methyl bendings $\delta(CH_3)$ make any assignment hazardous without the assistance of calculations. Indeed, $(Ca^{2+}, AcO^-)(H_2O)_{n=0-3}$ and $(Ba^{2+}, AcO^-)(H_2O)_{n=0-5}$ clusters present complex patterns in the 1350-1575 cm^{-1} spectral range. However, the isolated intense transition lying around 1520-1550 cm^{-1} for $(Ca^{2+}, AcO^-)(H_2O)_{n=4-8}$ clusters can be safely assigned to $\nu_a(CO_2^-)$ based on previous works.[19, 20] By extrapolation, the blue-most intense transitions in this 1350-1575 cm^{-1} spectral range for the other clusters are tentatively assigned to $\nu_a(CO_2^-)$, which will be further confirmed by calculations. Remarkably, a blue-shift of these $\nu_a(CO_2^-)$ transitions is observed along both series (Fig. 3), but with significantly different behaviors: a rather constant blue-shift for the Ca^{2+} series with a notable exception between n=4 and n=5, vs. a rapid increase followed by a plateau from n=2 for Ba^{2+}. The number and relative intensities of $\delta(H_2O)$ transitions appear also to be quite different for n=3-5 clusters. These observations evidence two significantly different microsolvation schemes, which need to be identified by a dedicated theoretical study.

[a] *LIDYL, CEA, CNRS, Université Paris Saclay*
CEA Saclay, Bât 522, 91191 Gif-sur-Yvette, France.
E-mail : eric.gloaguen@cea.fr
[b] *Laboratory for Chemistry and Life Science, Tokyo Institute of Technology, Yokohama 226-8503, Japan.*
E-mails: ishiuchi.s.aa@m.titech.ac.jp, mfujii@res.titech.ac.jp

†Electronic Supplementary Information (ESI) available: Experimental Methods; Theoretical methods; Structures. See DOI: 10.1039/x0xx00000x

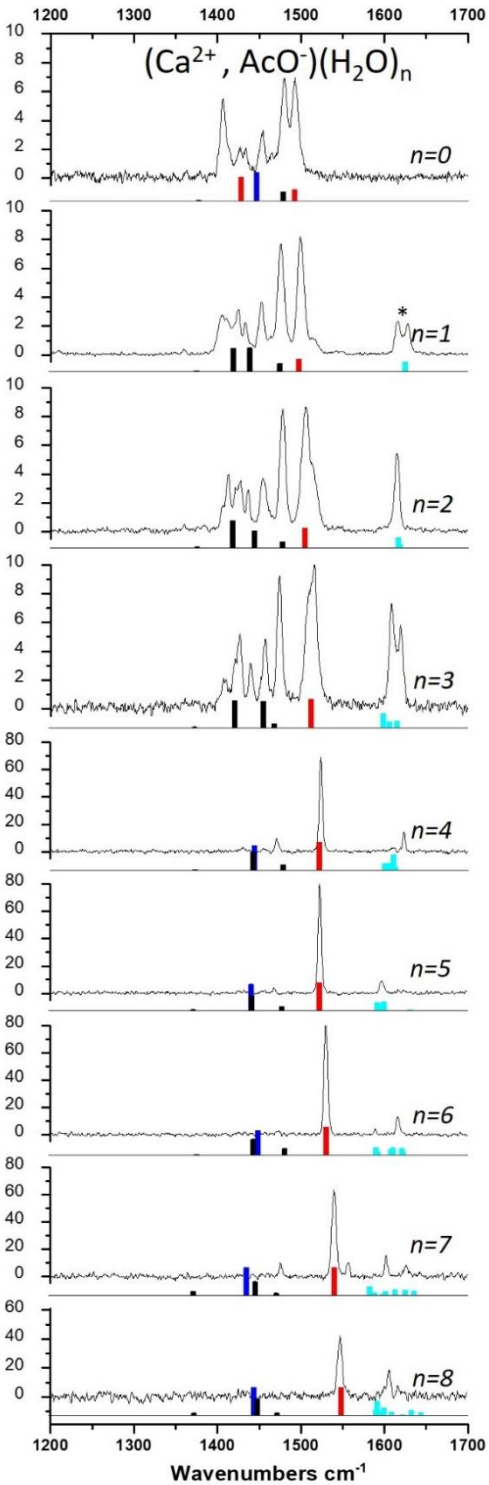

Figure 1. Experimental IR spectra of H_2-tagged (Ca^{2+}, AcO^-)$(H_2O)_{n=0-8}$ clusters. For each spectrum, the total integrated intensity has been set to match the sum of the calculated intensities on the 1200-1700 cm^{-1} range (Fig. S2). Scaled harmonic frequencies (stick spectra) are also shown for comparison purposes. The vibrational mode assignment resulting from a normal mode analysis (Section S2) is shown by a color code: $\nu_a(CO_2^-)$ (red); $\nu_s(CO_2^-)$ (blue); $\delta(H_2O)$ (cyan); other (black). (*) marks a doublet which may result from anharmonic couplings[23] or tunneling splitting.[24, 25]

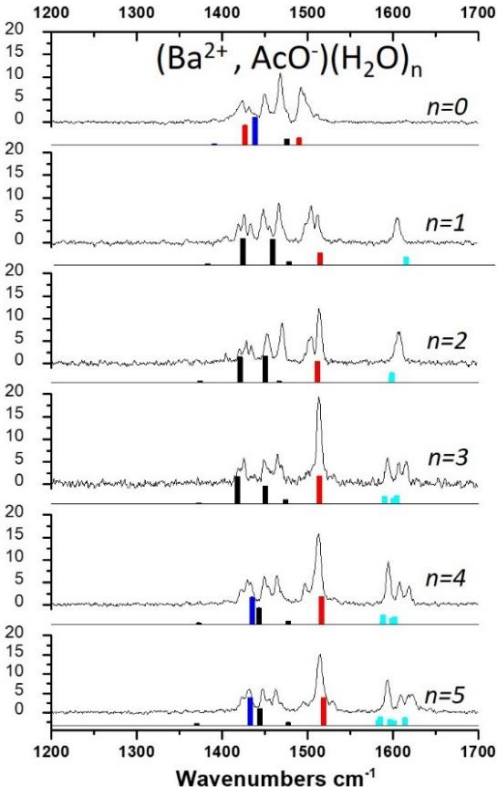

Figure 2. Experimental IR spectra of H_2-tagged (Ba^{2+}, AcO^-)$(H_2O)_{n=0-5}$ clusters. Same legend as Figure 1.

In order to find theoretical structures capable to match the observations, we optimized the geometry and calculated the harmonic vibrational frequencies of 106 (resp. 82) structures for Ca^{2+}-containing (resp. Ba^{2+}) clusters at the RI-B97-D3/dhf-TZVPP level, including H_2 tags in our calculations (Section S2). Then, we assigned the experimental spectra to these structures according to two reliable criteria: (i) the frequency of $\nu_a(CO_2^-)$ and $\delta(H_2O)$ transitions ; (ii) the number and intensity of the $\delta(H_2O)$ transitions up to n=5, the decrease of the signal-to-noise ratio making this criterion less reliable from n=6. Interpretation of the coupled $\nu_s(CO_2^-)$ and $\delta(CH_3)$ modes would demand, for their part, an appropriate theoretical treatment of anharmonic effects,[26-28] which is out of the scope of this study. Consequently, the corresponding spectral range displays obvious differences between experiments and simulations, and is thus not exploited for assignment purposes. The assigned structures are shown in Fig. 4 and 5, and their calculated frequencies are reported in Fig. 1, 2 and 3 together with the vibrational mode assignment resulting from the vibrational analysis (Section S2). The agreement between both experimental and theoretical datasets is not only quite satisfactory for each structure according to the above-mentioned criteria (Fig. 1 and 2), but is also very good when considering the evolution along the series (Fig. 3).

Focusing first on (Ca^{2+}, AcO^-)$(H_2O)_n$ clusters (Fig. 4), the microsolvation scheme can be decomposed as a function of n. For n=1-4, one observes that water molecules fill the first solvation shell of calcium, and stay too far from the carboxylate group to make strong H-bonds (Fig. 6), forming at best an elongated H-bond for n=4 (229 pm). Then, the fifth water

molecule starts to fill the second solvation shell of calcium. Finally, for n ≥ 6, water molecules fill both the second solvation shell of calcium and much better the first shell of carboxylate than the previous molecules (H-bonds shorter than 200 pm), thus making a H-bond network around the ion pair.

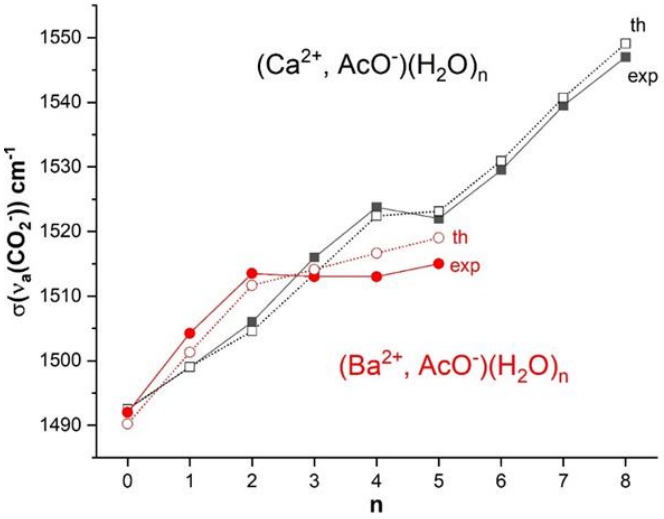

Figure 3. Experimental (solid symbols) and theoretical (open symbols) wavenumbers σ of $\nu_a(CO_2^-)$ for $(Ca^{2+}, AcO^-)(H_2O)_{n=0-8}$ (black squares) and $(Ba^{2+}, AcO^-)(H_2O)_{n=0-5}$ (red circles) clusters.

As already observed for $(Ca^{2+}, d\text{-}PrO^-)(H_2O)_n$,[20] several spectroscopic trends accompany this microsolvation scheme, *e.g.* a red-shift of $\delta(H_2O)$ and a blue-shift of $\nu_a(CO_2^-)$ transitions. Remarkably, the blue-shift induced by hydration has a spectacular effect on the coupling of $\nu_a(CO_2^-)$ with $\delta(CH_3)$: while the intensity of $\nu_a(CO_2^-)$ is spread over several transitions for n=0-3 due to a strong coupling, this coupling suddenly disappears due to the on-going blue-shift of the $\nu_a(CO_2^-)$ transition, which becomes intense and sharp for n ≥ 4. $\nu_a(CO_2^-)$ has also proven to be an indicator of the ionic bond strength in bidentate species: (i) an increase of the splitting $\Delta\nu_{a\text{-}s}(CO_2^-)$ together with a blue-shift of $\nu_a(CO_2^-)$ have been observed for carboxylate groups paired with alkali cations of increasing size, revealing the relaxation of the carboxylate group resulting from the weakening of the ionic bond;[9] (ii) a blue-shift of $\nu_a(CO_2^-)$ is also observed when the cation is simultaneously involved in a competing cation-π interaction, weakening the ionic bond.[15] Similarly, $\nu_a(CO_2^-)$ can be used in this microsolvation study to trace the effect of the carboxylate binding partners, *i.e.* both the cation and water molecules. The blue-shift observed for n=0-4 and n=5-8 (Fig. 3) reflects the gradual weakening of the ionic bond induced by hydration, which is also monitored by the increase of the cation-anion distance (Fig. 6). The fact that water molecules make efficient H-bonds (n=5-8) or not (n=0-4) has no real impact on the relaxation of the carboxylate group, which is dominated by the motion away of the cation. The passage from n=4 to n=5 is an exception, as the fifth water molecule goes to the second shell of the cation, which induces neither a blue-shift (Fig. 3) nor a significant increase of the cation-anion distance (Fig. 6). Interestingly, this characteristic "stop" of the blue-shift at n=5 has also been observed in $(Ca^{2+}, d\text{-}PrO^-)(H_2O)_n$ experimental spectra,[20] but has not been assigned to the addition of the fifth water molecule to the second solvation shell of calcium. However, IR spectra of $(Mg^{2+}, AcO^-)(H_2O)_{n=0-5}$ Sup. Info. of ref. 19 in the OH stretch region show that strong H-bonds are indeed created at n=5, supporting a microsolvation scheme for this system similar to that proposed here for $(Ca^{2+}, AcO^-)(H_2O)_n$ clusters.

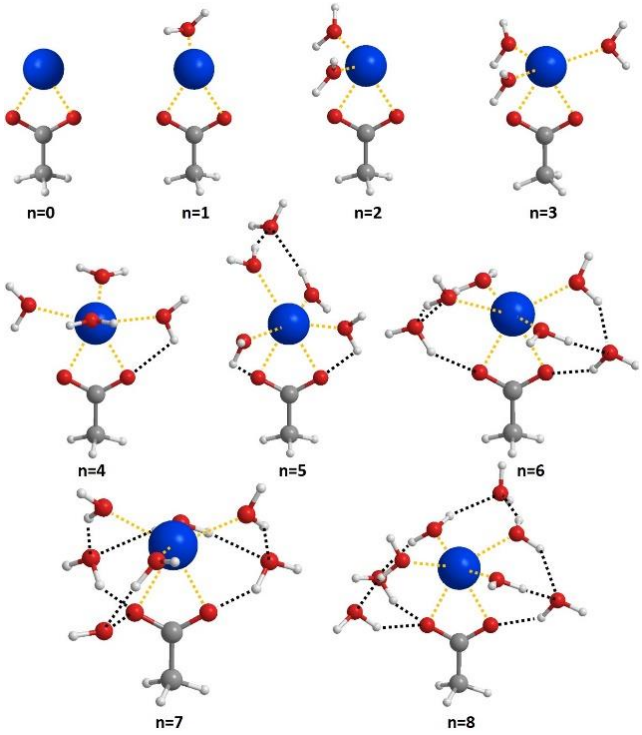

Figure 4. RI-B97-D3/dhf-TZVPP theoretical structures of $(Ca^{2+}, AcO^-)(H_2O)_{n=0-8}$ clusters (H_2 tags not shown). H-bonds (< 240 pm) are shown by black dotted lines, while the cation is linked to its first solvation shell by orange dotted lines.

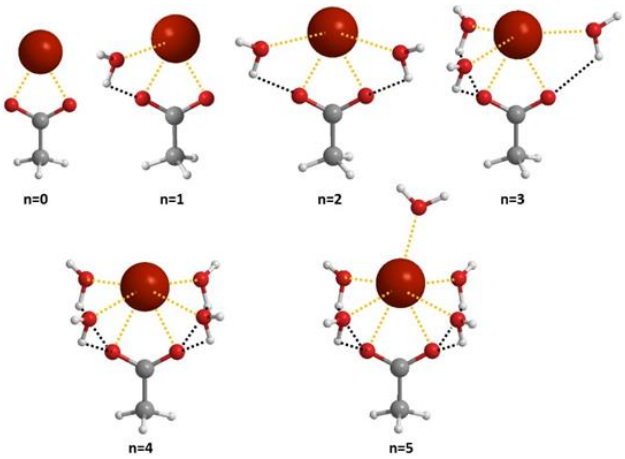

Figure 5. RI-B97-D3/dhf-TZVPP theoretical structures of $(Ba^{2+}, AcO^-)(H_2O)_{n=0-5}$ clusters (H_2 tags not shown). Same legend as Figure 4.

Regarding $(Ba^{2+}, AcO^-)(H_2O)_n$ clusters (Fig. 5), the microsolvation scheme up to n=5 consists of adding molecules in the first solvation shell of barium. The first four water molecules make simultaneously elongated H-bonds with carboxylate (214 <

d($CH_3CO_2^-$···HOH) < 237 pm, Fig. 6), and the fifth one lies opposite to acetate. Taking again $\nu_a(CO_2^-)$ as an indicator of the interactions of carboxylate with its binding partners, Fig. 3 suggests that the strong blue-shift induced by the first two water molecules correspond to a significant weakening of the ionic bond. However, additional water molecules (n=3-5) induce no additional blue-shift whereas the cation continues to move away from the carboxylate group (Fig. 6). As a consequence, the $\nu_a(CO_2^-)$ transition remains coupled to $\delta(CH_3)$ up to n=5 for (Ba^{2+}, AcO^-)$(H_2O)_n$ clusters, displaying a marked difference with (Ca^{2+}, AcO^-)$(H_2O)_n$ clusters (Fig. 1 and 2). The weakening of the ionic bond expected from the increase of the cation-anion distance (Fig. 6) thus appears in contradiction with the plateau observed for the $\nu_a(CO_2^-)$ transition. This fact can be explained if one considers that the water molecules binding to carboxylate compensate the motion away of the cation, resulting in a globally unrelaxed carboxylate group between n=2 and n=5.

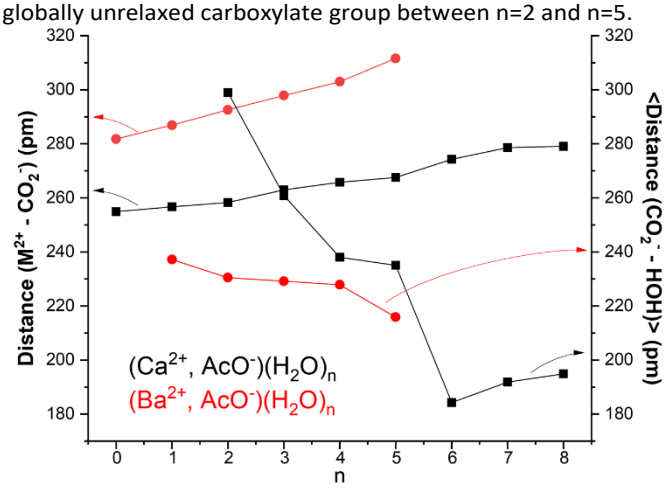

Figure 6. Evolution of intermolecular distances in (Ca^{2+}, AcO^-)$(H_2O)_{n=0-8}$ (black) and (Ba^{2+}, AcO^-)$(H_2O)_{n=0-5}$ (red) clusters. Left axis: metal ion M^{2+}-CO_2^- interatomic distance (cation-anion distance) ; right axis: H-bonds to acetate (value averaged over all the H-bonds).

These microsolvation schemes provide clues about the respective role of water molecules in solvating these ion pairs. The primary role of the first water molecules is to solvate the divalent cations in both cases, the evolution of the H_2O-cation distances being qualitatively the same as that observed for the hydrated cations.[29] However, water molecules interact with acetate stronger and earlier in the microsolvation scheme when paired with Ba^{2+} compared to Ca^{2+} (H-bond lengths to acetate, Fig. 6), which can be seen as a direct consequence of the larger ionic radius of the former cation: the relatively weaker electrostatic interaction with Ba^{2+} release water molecules, which can bind more efficiently to acetate. In parallel, the cation-anion distance increases faster for Ba^{2+} than for Ca^{2+} (Fig. 6), showing that water molecules, by interacting simultaneously with both the cation and the anion, have a greater dissociation efficiency in the former case.

Two mechanisms involved in the ion dissociation emerge from these microsolvation schemes. In the first one, water molecules mainly solvate the cation, which, in turn, gradually become a relatively worse partner for an ionic bond with acetate like for other water molecules[29] or any other ligand. Thus, water molecules play here an indirect role in the weakening of the ionic bond. This mechanism, not specific to ion pairs, is at play for both cations investigated, and appears as the first driving force of the first stages of ion dissociation. In the case of Ba^{2+}, however, water molecules also bind simultaneously to the cation and the acetate group (Fig. 5), which may be seen as the beginning of the insertion of water in between the ions. This specific mechanism reveals a more direct role of water molecules in the ion dissociation, and has already been documented for other types of pairs such as alkali halide[13, 17] or alkali acetate.[18] Interestingly, this mechanism is barely observed for Ca^{2+} (Fig. 4), even when water strongly binds to acetate (n=6-8): none of these H-bond donor water molecules belong to the first solvation shell of Ca^{2+}, highlighting the stability of this contact ion pair upon microsolvation. Furthermore, one should mention the non-intuitive reading of IR spectra. While the first mechanism is associated with a constant blue-shift of the $\nu_a(CO_2^-)$ transition, the second mechanism tends to cancel this effect, ending in a steady position of the $\nu_a(CO_2^-)$ transition. The IR spectra of *e.g.* n=5 clusters (Fig. 1-3) thus show a carboxylate group more strongly bound to its partners for Ba^{2+} than for Ca^{2+}, whereas the ions are more dissociated in the former case as illustrated by a steeper increase of the cation-anion distance between n=0 and n=5 (Fig. 6). This example illustrates once more the difficulty to disentangle the respective effects of the counter-ions and the surrounding water molecules on the spectroscopy of carboxylate.

Finally, the frequency of the $\nu_a(CO_2^-)$ transition of free acetate ions, 1551.5 cm^{-1},[10] is almost reached for (Ca^{2+}, AcO^-)$(H_2O)_8$ clusters (1547 cm^{-1}), despite the fact that ions are far from being fully dissociated. This result echoes that of Denton et al. for (Ca^{2+}, *d*-PrO^-)$(H_2O)_{12}$ clusters, illustrating the difficulty to follow the complete dissociation process by IR spectroscopy, as already reported for alkali cations.[9, 10] Consequently, the investigation of larger clusters by this approach should be carried out at an advanced theoretical level capable to reproduce experimental frequencies with an accuracy close to the wavenumber scale.

Conflicts of interest

There are no conflicts to declare.

Acknowledgments

JD, SII, MF and EG acknowledge the JSPS Summer program 2018. JD, JXB, VB and EG acknowledge ANR (grants IONPAIRS ANR-16-CE29-0017 and VAPOBIO ANR-20-CE29-0016). SII and MF acknowledge KAKENHI grants JP18H01938, JP19H05527, JP19K23624, JP20H00372 and JP21H04674, World Research Hub Initiative in Tokyo Institute of Technology, Cooperative Research Program of the ''Network Joint Research Center for Materials and Devices'' from the Ministry of Education, Culture, Sports, Science and Technology (MEXT).

Notes and references

1. Y. Marcus and G. Hefter, *Chem. Rev.*, 2006, **106**, 4585.
2. K. D. Collins, *Biophys. Chem.*, 2012, **167**, 43.
3. P. Jungwirth, *J. Phys. Chem. B*, 2014, **118**, 10333.
4. N. F. A. van der Vegt, K. Haldrup, S. Roke, J. R. Zheng, M. Lund and H. J. Bakker, *Chem. Rev.*, 2016, **116**, 7626.
5. B. Hess and N. F. A. van der Vegt, *Proc. Natl. Acad. Sci. U. S. A.*, 2009, **106**, 13296.
6. E. F. Aziz, N. Ottosson, S. Eisebitt, W. Eberhardt, B. Jagoda-Cwiklik, R. Vacha, P. Jungwirth and B. Winter, *J. Phys. Chem. B*, 2008, **112**, 12567.
7. J. S. Uejio, C. P. Schwartz, A. M. Duffin, W. S. Drisdell, R. C. Cohen and R. J. Saykally, *Proc. Natl. Acad. Sci. U. S. A.*, 2008, **105**, 6809.
8. W. W. Rudolph, D. Fischer and G. Irmer, *Dalton trans.*, 2014, **43**, 3174.
9. S. Habka, T. Very, J. Donon, V. Vaquero-Vara, B. Tardivel, F. Charnay-Pouget, M. Mons, D. J. Aitken, V. Brenner and E. Gloaguen, *Phys. Chem. Chem. Phys.*, 2019, **21**, 12798.
10. J. Donon, S. Habka, T. Very, F. Charnay-Pouget, M. Mons, D. J. Aitken, V. Brenner and E. Gloaguen, *Chemphyschem*, 2021, **22**, 2442.
11. D. Strasser, F. Goulay, M. S. Kelkar, E. J. Maginn and S. R. Leone, *J. Phys. Chem. A*, 2007, **111**, 3191.
12. R. Cooper, A. M. Zolot, J. A. Boatz, D. P. Sporleder and J. A. Stearns, *J. Phys. Chem. A*, 2013, **117**, 12419.
13. R. Z. Li, C. W. Liu, Y. Q. Gao, H. Jiang, H. G. Xu and W. J. Zheng, *J. Am. Chem. Soc.*, 2013, **135**, 5190.
14. C. J. Johnson, L. C. Dzugan, A. B. Wolk, C. M. Leavitt, J. A. Fournier, A. B. McCoy and M. A. Johnson, *J. Phys. Chem. A*, 2014, **118**, 7590.
15. S. Habka, V. Brenner, M. Mons and E. Gloaguen, *J. Phys. Chem. Lett.*, 2016, **7**, 1192.
16. A. M. Sadoon, G. Sarma, E. M. Cunningham, J. Tandy, M. W. D. Hanson-Heine, N. A. Besley, S. F. Yang and A. M. Ellis, *J. Phys. Chem. A*, 2016, **120**, 8085.
17. G. L. Hou, C. W. Liu, R. Z. Li, H. G. Xu, Y. Q. Gao and W. J. Zheng, *J. Phys. Chem. Lett.*, 2017, **8**, 13.
18. W. J. Zhang, G. L. Hou, P. Wang, H. G. Xu, G. Feng, X. L. Xu and W. J. Zheng, *J. Chem. Phys.*, 2015, **143**, 054302.
19. J. W. DePalma, P. J. Kelleher, L. C. Tavares and M. A. Johnson, *J. Phys. Chem. Lett.*, 2017, **8**, 484.
20. J. K. Denton, P. J. Kelleher, M. A. Johnson, M. D. Baer, S. M. Kathmann, C. J. Mundy, B. A. W. Rudd, H. C. Allen, T. H. Choi and K. D. Jordan, *Proc. Natl. Acad. Sci. U. S. A.*, 2019, **116**, 14874.
21. J. R. Rumble, *Journal*, 2021.
22. K. D. Collins, *Biophys. Chem.*, 2006, **119**, 271.
23. J. A. Davies, M. Mugglestone, S. F. Yang and A. M. Ellis, *J. Phys. Chem. A*, 2020, **124**, 6528.
24. K. Kuyanov-Prozument, M. Y. Choi and A. F. Vilesov, *J. Chem. Phys.*, 2010, **132**.
25. A. Kilaj, H. Gao, D. Rosch, U. Rivero, J. Kupper and S. Willitsch, *Nat. Commun.*, 2018, **9**.
26. S. Bakels, M. P. Gaigeot and A. M. Rijs, *Chem. Rev.*, 2020, **120**, 3233.
27. H. Otaki, K. Yagi, S. Ishiuchi, M. Fujii and Y. Sugita, *J. Phys. Chem. B*, 2016, **120**, 10199.
28. P. T. Panek and C. R. Jacob, *Chemphyschem*, 2014, **15**, 3365.
29. A. L. Derepas, J. M. Soudan, V. Brenner, J. P. Dognon and P. Millié, *J. Comput. Chem.*, 2002, **23**, 1013.